Cod: 3.1001

CHLORINE AND COPPER ANALYSES TO THE EFFECT OF THE MOLECULAR STRUCTURE OF CARBON ON THE MECHANISM OF CHLORINATION

A. Toda[1], T. Fujimori[1], K. Shiota[1], M. Takaoka[1]
[1]*Kyoto University*

INTRODUCTION

The specific properties of macromolecular carbon in municipal solid waste incineration fly ash, such as the surface area, functional groups, and free radicals, influence the thermochemical formation of polychlorinated dibenzo-p-dioxins and furans (PCDD/Fs), polychlorinated biphenyls (PCBs), and chlorobenzenes (CBzs).[1] The molecular structure of carbon also influences the formation of these chemicals.[2] One study suggested that different paths lead to the thermochemical formation of different carbon nanomaterials.[2] Recently, various carbon nanomaterials with advantageous electrical, mechanical, and optical properties have been developed to alter their functional properties.[3] In the future, these carbon nanomaterials may be incinerated with municipal solid waste. In this study, we made model samples from carbon nanomaterials and conducted X-ray absorption near edge structure (XANES) experiments and examined the differences in thermochemical changes in the chemical forms of chlorine and copper among different carbon nanomaterials.

MATERIALS AND METHOD

Model samples were made using six types of carbon: activated carbon (AC), graphite (G), graphene with a surface area of 300 m^2/g (Gra300) or 500 m^2/g (Gra500), single-wall carbon nanotubes (CNT), and fullerene (C60) (Table 1). We removed any organic compounds from the AC by heating it at 500°C for 60 min under a stream of 100% nitrogen gas (100 mL/min).[3] Each model sample included a carbon (50 wt%) and metal catalyst ($CuCl_2$, 50 wt%). After the model sample was ground, we heated the mixture in a quartz boat at room temperature (RT), 200°C, 300°C, or 400°C for 30 min under a stream of 10% oxygen/90% nitrogen gas (50 mL/min). For Cu K-edge XANES measurements, a 200-mg model sample was pressed into a 13-mm-diameter disk [model samples (2.65% Cu) and boron nitride (BN; base material)]. Cu K-edge XANES was performed at SPring-8. The X-ray passed through the sample disk, and were collected in transmission mode with a Si(111) monochromator. Cl K-edge XANES was performed at the Photon Factory, with powdered samples mounted on carbon tape. XANES spectra were collected in total electron yield mode in a vacuum. The spectra of reference materials and the model sample were measured and normalized. We used linear combination fitting (LCF) to compare the normalized spectra and to determine the major species using the software REX2000. The reference species used for the XANES analyses are shown in Fig.1. LCF of the references to the model samples was performed [Cl: 2,815~2,825, ~2,830, ~2,840, and ~2,850 eV and Cu: 8,970~9,040, ~9,060, and ~9,080eV] and the results were averaged (Table 2).

RESULTS

Dynamic changes in the chemical forms of Cl and Cu in the model samples were observed by XANES (Table 2, Fig. 3); the higher the temperature, the more $CuCl_2$ was reduced to CuCl, except for AC at 400°C and C60. At higher temperatures, such as for AC at 400°C, CuCl was converted into oxychloride compounds such as $Cu_2(OH)_3Cl$, and the percentage of CuCl decreased. When reduction occurred (i.e., $CuCl_2 \rightarrow CuCl$), chlorinated aromatics (Aroma-Cl) appeared. This behavior is consistent with the oxychlorination cycle of Cu (Figs. 2 and 3).[4, 5]

The effect of temperature and extent of dechlorination differed considerably according to the carbon source. For G, there was little Cl and Cu in the forms of PCDD/Fs, PCBs, and CBzs, and changing the temperature had little effect on the concentrations (Fig. 4). At each temperature, most of the Cl in G was $CuCl_2$ by LCF. For AC heated at 400°C, the CuCl reacted to form $Cu_2(OH)_3Cl$ (39%, Cl K-edge; 41%, Cu K-edge), so we propose that AC goes through a step in the oxychlorination cycle at low temperatures. Since AC has many reactive sites at its edges, AC readily reacts with a catalyst, such as Cu.

The extent of $CuCl_2$ dechlorination and the surface area of the carbon materials was in the order AC > Gra500 > Gra300 > G. From this, we suggest that the molecular structure of carbon, i.e., sheet-like

(Gra300 and Gra500), layered (G), cylindrical (CNT), and ball-like (C60) structures, plays a dominant role in the oxychlorination cycle.

Unlike the AC used by previous study[4, 5], the CNT and C60 showed great changes at 300–400°C. The Cl K-edge XANES spectra of C60 indicated that although the chemical form of the C60 model sample heated at RT, 200°C, and 300°C changed little, 64% of the Cl was aromatic in carbons (Aroma-Cl) at 400°C (Fig. 3).

The Cl concentration can be reliably measured with high sensitivity using XANES.[6] Therefore, we calculated the Cl concentration from the energy jump in the XANES spectra at 2,850.8 eV (Table 3, Fig. 4). However, the Cl concentration was outside the range reported by Leri et al.[6] We compared the Aroma-Cl concentration with the concentrations of PCDD/Fs, PCBs, and CBzs (Fig. 5). The CBzs concentration was positively correlated (R^2 = 0.8975) with the Aroma-Cl concentration in Leri et al.6 although the composition of the model sample differed a little from that in another study[2].

All of the Cl concentrations increased at RT through 200°C (Fig. 4). The dewatering process that occurs at around 100°C might reduce the total amount of the model sample, increasing the concentration. The Cl concentrations at 400°C were higher that at the other temperatures. In a previous study,[2] after heating the model sample (50 wt% carbon, 50 wt% $CuCl_2$#$2H_2O$) at 300°C, the total organic carbon decreased more than in the unheated sample (RT). The residual ratio of the heated sample [AC (77.7%) > Gra500 (93.1%) > G (93.6%) > Gra300 (93.7%)] suggested that CO_2 gas emitted decreases the carbon concentration, indirectly causing the increase in the Cl concentration. The Cl concentration sometimes decreased. Some chlorinated gas, such as HCl, might be released during the thermochemical process, resulting in the decrease in the total Cl concentration.

In conclusion, although graphene, CNT, and C60 are carbon allotropes, the molecular structure of carbon plays an effective role not only on the dechlorination of $CuCl_2$ but also in the change in the total Cl concentration.

ACKNOWLEDGEMNT

We thank Dr. KITAJIMA for helping at Photon Factory, and Dr. URUGA at SPring-8, and financial support by a Grand-in-Aid for Young Scientist (A) (26701012) and for Scientific Research (B) (25289171) from JSPS, MEXT, Japan, and Grant for Environmental Research Projects from the Sumitomo Foundation, Japan (123120).

REFERENCE

1. Fujimori T, et al. (2014); Aerosol and Air Qual Res. 14: 1131-41
2. Fujimori T, et al. (2015); Dioxin 2015, 34th International Symposium on Halogenated Persistent Organic Pollutants
3. Zhu Y, et al. (2010); Adv Mater. 22: 3906-24
4. Takaoka M, et al. (2005); Environ. Sci. Technol. 39: 5878-5884
5. Fujimori T et al. (2009); Environ. Sci. Technol. 43: 2241-2246
6. Leri A.C, et al (2006); Anal. Chem. 78: 5711-5718

Table.1 The grade of carbon nanomaterials

	Surface Area (m^2/g)	purity (%)	manifacture
AC	1530	*	Takeda Chemical Industries
Gra300	500	99.5	Strem Chemicals
Gra500	300	99.5	
G	8.8	98	Wako Pure Chemical Industries
CNT	*	93; chirality (6,5)	Sigma-Aldrich
C60	*	>99.9	Strem Chemicals

*; not measured

Table.2 The percentages of the chemical forms relative to the total Cl and total Cu

		Percentages Relative to Cl K-edge(%)					Percentages Relative to Cu K-edge(%)						
	Temp(℃)	CuCl	$CuCl_2$	Alipha-Cl	$Cu_2(OH)_3Cl$	Aroma-Cl	CuCl	$CuCl_2$	CuO	Cu_2O	Cu	$Cu_2(OH)_3Cl$	$Cu(OH)_2$
AC	rt	<5*	**94**		<5*	<5*		**93**	<5	<5*	<5*		<5*
	200	13*	**83**	<5*		<5*		**94**	<5				<5
	300	**48***	33*		<5*	13	**50**	22				15	13
	400	**42***	4.6*		39*	14*	14	29	5.7	<5		**41**	9.4
C60	rt	<5	**96**					**93**				<5*	<5*
	200	5.2	**94**			<5*		**97**				<5*	<5
	300	6.5	**84**	<5*		8.5*		**94**				<5*	<5
	400		21*	15*		**64***	**50**	43					7.4
CNT	rt	6.8*	**91**			<5*		**96**	<5				<5
	200	9.4	**86**		<5*	<5*	<5	**89**		5.6	<5*		
	300	7*	**91**	<5*		<5*	15	**74**	<5	6.7			
	400	**66***	8.9*		13*	12	**50**	22				15	13
G	rt	<5*	**95**			<5*		**99**	<5		<5*		
	200	9.6*	**87**			<5*		**99**	<5				
	300	5.5*	**85**		9.5*		<5	**99**					
	400	18	**81**	<5*		<5*	16	**82**					<5
Gra300	rt	5.4*	**86**		<5*	6.8*		**96**	<5				<5*
	200	<5*	**73**		9.1*	14		**95**	<5		<5		
	300	15*	**71**		7.3*	7.4*	10	**78**	<5*			<5*	9
	400	35*	**42**		14*	8.5*	**50**	35				6.2	8.9
Gra500	rt	8.1*	**78**	<5*	<5*	9.9*		**95**	<5	<5			
	200	9.6*	**64**		5.2*	21		**95**	<5				
	300	18*	**63**		<5*	14*	15	**73***	<5*			<5	8.3
	400	**48***	32		<5*	17	**41**	31				19	8.7

*; coefficient variation is >5%

Table.3 The concentration of Cl expected from the difference at 2850.8eV between splines through the pre-edge and post-edge region

		Cl-ppm by XAFS analysis					
	Temp(℃)	CuCl	$CuCl_2$	Alipha-Cl	$Cu_2(OH)_3Cl$	Aroma-Cl	TOTAL
AC	rt	8000	240000	210	3100	4400	260000
	200	46000	280000	660	0	12000	340000
	300	140000	96000	0	15000	38000	280000
	400	160000	17000	0	140000	54000	370000
C60	rt	6000	130000	0	0	0	140000
	200	16000	280000	0	0	880	300000
	300	7200	94000	1900	0	9400	110000
	400	0	73000	50000	0	220000	350000
CNT	rt	14000	190000	0	0	5400	210000
	200	27000	240000	0	770	11000	280000
	300	20000	260000	1500	0	3100	270000
	400	270000	36000	0	51000	48000	400000
G	rt	5100	110000	0	0	120	110000
	200	21000	190000	0	0	6300	220000
	300	11000	180000	0	20000	0	210000
	400	87000	380000	950	0	3600	470000
Gra300	rt	8600	140000	0	3000	11000	160000
	200	8900	150000	0	19000	29000	210000
	300	50000	240000	0	25000	25000	340000
	400	120000	150000	0	48000	30000	350000
Gra500	rt	9900	95000	1200	6300	12000	120000
	200	28000	190000	0	15000	61000	290000
	300	49000	170000	0	12000	38000	270000
	400	190000	120000	0	13000	64000	390000

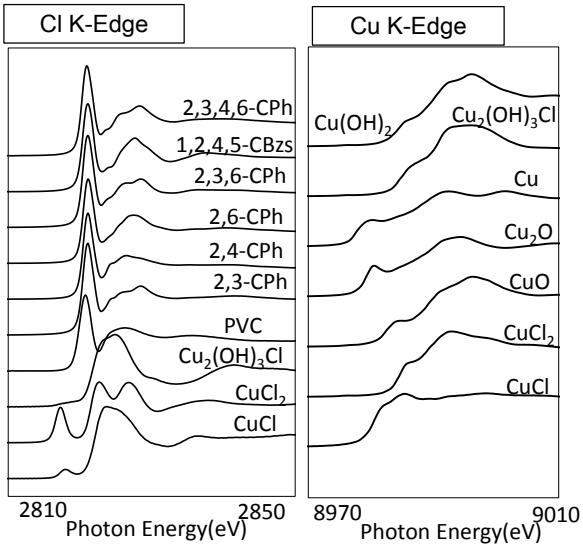

Fig.1 Cu and Cl K-edge X-ray absorption near edge structure (XANES) spectra of a standard sample

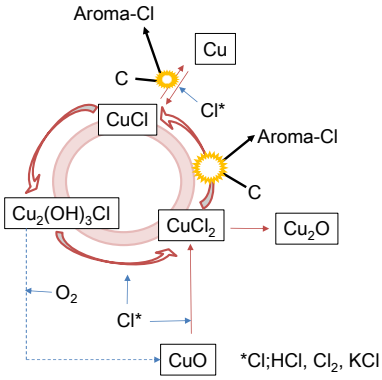

Fig.2 The oxychlorination cycle of copper in fly ash[4]

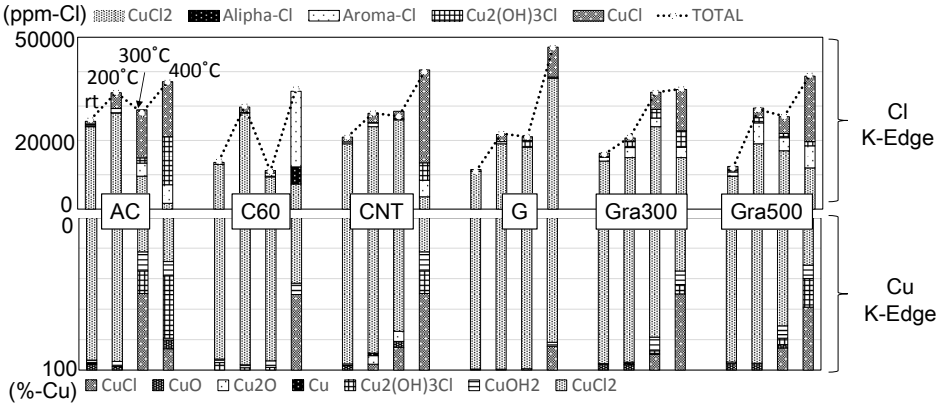

Fig.3 The chemical forms of Cl and Cu (%) at each temperature based on linear combination fitting of XANES, and the concentration of Cl

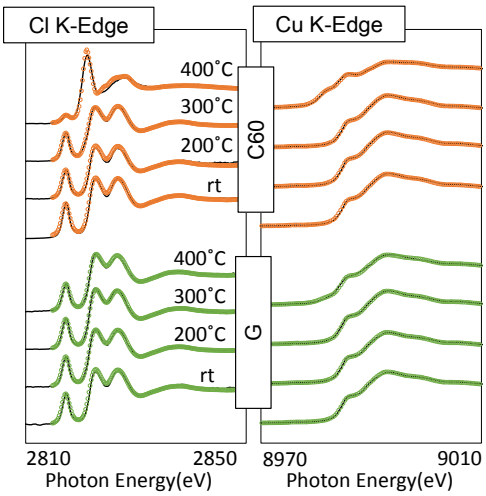

Fig.4 Cl and Cu K-edge XANES spectra of model samples (G and C60) heated at 400˚C, 300˚C, 200˚C, and room temperature (RT)

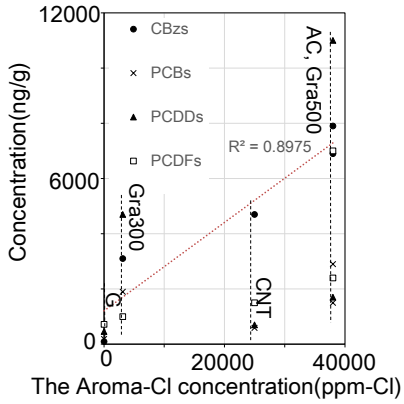

Fig.5 Relationship between the concentration of PCDD/Fs, PCBs, and CBzs and the Aroma-Cl concentration by XAFS analysis